Marine and Petroleum Geology 60 (2015) 79–86

Contents lists available at ScienceDirect

Marine and Petroleum Geology

journal homepage: www.elsevier.com/locate/marpetgeo

Research paper

# Carbon isotopic fractionation by desorption of shale gases

Xiaofeng Wang [a, *], Xiaofu Li [a, b], Xiangzeng Wang [c], Baoguang Shi [a], Xiaorong Luo [a], Lixia Zhang [c], Yuhong Lei [a], Chengfu Jiang [c], Qiang Meng [a, b]

[a] Key Laboratory of Petroleum Resources, Gansu Province/Key Laboratory of Petroleum Resources Research, Institute of Geology and Geophysics, Chinese Academy of Sciences, Lanzhou 730000, PR China
[b] University of Chinese Academy of Sciences, Beijing 100049, PR China
[c] Shaanxi Yanchang Petroleum (Group) CO., LTD., Xi'an 710075, PR China

ARTICLE INFO

*Article history:*
Received 7 May 2014
Received in revised form
17 November 2014
Accepted 26 November 2014
Available online 4 December 2014

*Keywords:*
Shale gas
Carbon isotopic composition
Adsorption/desorption
Adsorption capacity

ABSTRACT

Geochemical studies of shale gas and conventional reservoirs within the Triassic Yanchang Formation of Xiasiwan and Yongning Field, Ordos Basin show that methane is isotopically depleted in $^{13}C$ as compared to $\delta^{13}C_1$ calculated by the Ro based on the relationship between $\delta^{13}C_1$ and Ro. Geochemical fractionation during the adsorption/desorption process of shale system may play a significant part in influencing $\delta^{13}C_1$ values of shale gas. Two shale core samples from confined coring of the Yanchang Formation were adopted segmented desorption experiments to examine this phenomenon. The results show that the $\delta^{13}C_1$ of desorbed gas changes little in the first few phases of the experiments at low desorption levels, but become less negative rapidly when the fraction of desorbed methane exceeds 85%. The desorption process for the last 15% fraction of the methane from the shale samples shows a wide variation in $\delta^{13}C_1$ from −49‰ to −33.9‰. Moreover, $\delta^{13}C_1$ of all desorbed methane from the shale samples is substantially depleted in $^{13}C$ than that calculated by Ro, according to Stahl and Carey's $\delta^{13}C_1$–Ro equation for natural gas generated from sapropelic organic matter. This shows some gases with isotopically enriched in $^{13}C$ cannot be desorbed under the temperature and pressure conditions of the desorption experiments. This observation may be the real reason for the $\delta^{13}C_1$ of shale gases and conventional reservoirs becomes more negative in Xiasiwan and Yongning Fields, Ordos Basin. The magnitude of the deviation between the $\delta^{13}C_1$ of shale gas and that calculated by Ro may be related to the adsorption capacity of shale or the proportion of absorbed gases. In this way, we may be able to evaluate the relative adsorption capacity of shale in geological conditions by $\delta^{13}C_1$ of the shale gas, or by $\delta^{13}C_1$ of conventional gas which generated by the shale with certainty. The $\delta^{13}C_1$ of conventional gas in Dingbian and Yingwang Fields have no deviation because the TOC value of the hydrocarbon source rock is relatively low.



## 1. Introduction

Shale gas is an important unconventional hydrocarbon resource in which natural gas is found as absorbed gas within organic matter and on inorganic minerals, as free gas within fractures and intergranular porosity, and as dissolved gas in kerogen, oil and water (Schettler and Parmely, 1990; Martini et al., 1998). Organic rich shales (or mudstones) can act as both source and reservoir rocks for petroleum fluids in a shale gas system; the adsorption state of the gas plays a critical role in the success of shale as a gas reservoir (Martini et al., 1998). The development of shale gas reservoirs has depended on a combination of geological, geochemical and engineering studies (Montgomery et al., 2005). Geological and geochemical evaluations provide the most basic information for the exploration and development of shale gas reservoir projects, and in the development of gas generation models. Shale gas systems are of two distinct types: biogenic (or microbial) and thermogenic (Claypool, 1998), although there can also be mixtures of the two gas types (Jarvie, 2007). Distinguishing between microbial and thermogenic $CH_4$ is essential for natural gas exploration and production strategies and improved resource estimates (Osborn and McIntosh, 2010).

The chemical composition and carbon isotopic composition ($\delta^{13}C$) of hydrocarbons have been widely applied to the

* Corresponding author. Permanent address: Key Laboratory of Petroleum Resources Research, Institute of Geology and Geophysics, Chinese Academy of Sciences, 382 Donggang West Road, Lanzhou, 730000, PR China. Tel./fax: +86 931 496 0853.
*E-mail address:* wangxf@lzb.ac.cn (X. Wang).

http://dx.doi.org/10.1016/j.marpetgeo.2014.11.003
0264-8172/

geochemical study of conventional natural gases (Schoell, 1980, 1983, 1988; Xu, 1994; Berner and Faber, 1996; Cramer et al., 1998; Tang et al., 2000; Liu et al., 2007). Such studies are critical for constraining both the genesis of natural gases and correlations with gas sources. The $\delta^{13}C$ characteristics of gaseous alkane homologues are used to differentiate gas sources. Based on the observed relationship between measured $\delta^{13}C$ values of $CH_4$ ($\delta^{13}C_1$) and vitrinite reflectance of source rocks (Ro), various models have been built to estimate the thermal maturity of source rocks based on the $\delta^{13}C$ of associated natural gas. Stahl and Carey (1975) established first empirical relationships between the maturity of source rocks and the $\delta^{13}C_1$ of related gaseous hydrocarbons which generated by sapropelic organic matter (Stahl and Carey, 1975; Stahl, 1977). From then on, a variety of such empirical relationships has been developed serving as important tools to solve applied geological problems (Dai and Qi, 1989; Faber, 1987; Shen et al., 1988). But these equations have not too much difference compared to Stahl and Carey's. Later, Chung et al. (1988) theorized that gaseous alkanes were produced by irreversible decomposition of organic matter and deduced a relationship between the $\delta^{13}C$ of the gaseous components and their carbon numbers. If the source rock $\delta^{13}C$ is homogenous and the source rocks are decomposed under a single thermal stress, then a linear correlation should exist between $\delta^{13}C_n$ and $1/n$, where $n$ corresponds to the carbon number (Chung et al., 1988). This means that the $\delta^{13}C$ of the primary alkane gases increases (becomes less negative) as the molecular mass increases.

The geochemical characteristics of shale gas have a certain particularity compared to conventional natural gases. For example, the $\delta^{13}C$ of gaseous alkanes mostly shows a reversals in highly mature shale gases such as the Barnett, Haynesville, Fayetteville, Woodford, Marcellus, Horn River and Utica shales (Burruss and Laughrey, 2010; Tilly et al., 2011; Tilly and Muehlenbachs, 2013; Zumberge et al., 2012; Xia et al., 2013). However, little attention has been paid to the observation that the shale gas is isotopically depleted in $^{13}C$ as compared to $\delta^{13}C$ values calculated from the established relationship between $\delta^{13}C_1$ and Ro. In general, the generation of shale gas follows a mechanism that is similar to that of conventional gas, which means the origins of shale gas can also be biogenic, thermogenic or a mixture of the two. Therefore, the reasons for the geochemical particularities of shale gas may be mainly related to the storage stage. For this reason geochemical fractionation during the adsorption/desorption process of shale gas is very important. The main purpose of this paper is to explain the relative isotopic depletion in $^{13}C$ of the shale gas and to analyze its geological significance. We have studied dynamic changes in the geochemical characteristics of shale gas (on the basis of the process of desorption through a series of experiments) in order to distinguish the influence of adsorption/desorption on the $\delta^{13}C_1$ of shale gas.

## 2. Samples and experiments

### 2.1. Natural gas samples

7 samples were collected by using the high pressure cylinder from Xiasiwan Field, Ordos Basin, including 4 shale gas samples and 3 conventional natural gas samples. 10 additional samples of conventional gas were collected in other fields (Fig. 1). All gas samples

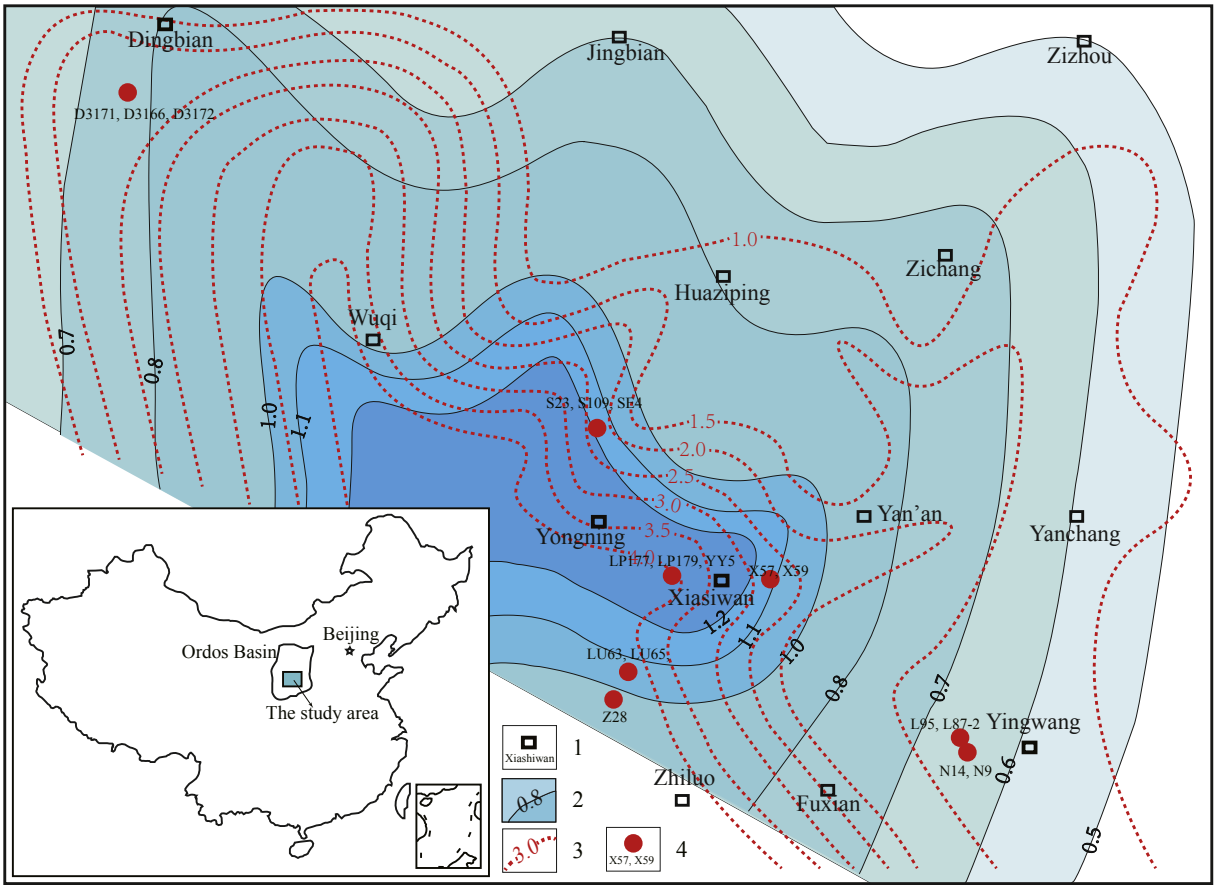


**Figure 1.** Map showing the geology of the study area and the sampling locations. 1. Place name, 2. Vitrinite reflectance isogram of the Chang 7, Yanchang formation (%Ro), 3. Total organic carbon isogram of the Chang 7, Yanchang formation (%). 4. Sampling location.

**Table 1**
Basic geochemical data of the shale core samples used in the desorption experiments.

| Name | Deep (m) | Weight | TOC (%) | Ro (%) | Tmax | S1 (mg/g) | S2 (mg/g) | IH (mg/gTOC) | IO (mg/gTOC) |
|---|---|---|---|---|---|---|---|---|---|
| YY5-1 | 1603–1605 | 1050 g | 5.57 | 1.1 | 455 | 3.94 | 0.29 | 184 | 5 |
| YY5-2 | 1603–1605 | 1210 g | 5.58 | 1.1 | 454 | 4.06 | 0.28 | 167 | 5 |

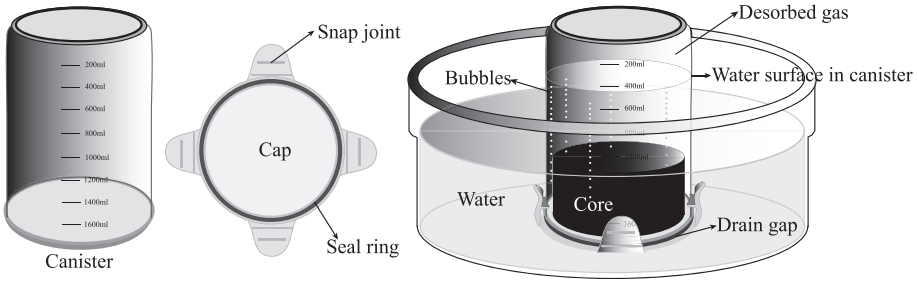


**Figure 2.** Schematic diagram of desorption experiments.

were analyzed in the Key Laboratory of Petroleum Resources Research, Institute of Geology and Geophysics, Chinese Academy of Sciences at Lanzhou.

### 2.2. Desorption experiments

Two shale core samples collected from confined coring of the Triassic Yanchang Formation in the Xiasiwan field (Fig. 1) were used in desorption experiments. The two samples were taken from the almost same depth in a single well and were initially subjected to the same step-wise desorption experiments (Table 1). The TOC values of the two shale core samples were 5.57%, 5.58% respectively, and the Ro was 1.1%. The samples are of 10 cm diameter, about 6 cm long, 1.05 kg and 1.21 kg in weight respectively. Shale core samples were immediately placed into a transparent sealed canister which filled with water and immersed upside down in water at the drilling site. Then cover the cap of the canister. Gas was observed to be given off gradually from the rock into the canister (Fig. 2). Gas desorption increased the pressure in the canister and caused a portion of the water to be expelled out by the gap in bottom of the canister. After 48 h, the core sample was removed from the canister and put into a new canister. The desorbed gas was collected in a glass bottle by discharging water. Its volume was measured and the material was tested for its chemical and isotopic composition. The core sample continued to desorb in the new canister for another 48 h, and the previous procedure was repeated 7 more times. The desorption experiment was divided into eight stages. Sampling was performed three times at 20 °C and subsequently at five elevated temperatures (40 °C, 60 °C, 70 °C, 80 °C, 90 °C). The conditions of the desorption experiments and gas analysis results are listed in Table 2.

### 2.3. Gas geochemical analysis

The chemical compositions of the gas samples were determined by Agilent 6890N gas chromatograph (GC) equipped with a flame ionization detector and a thermal conductivity detector. Individual hydrocarbon gas components from methane to pentane ($C_1$–$C_5$) were separated using a capillary column (PLOT $Al_2O_3$ 50 m × 0.53 mm). The GC oven temperature was initially set to 30 °C for 10 min, and then increased to 180 °C at 10 °C/minute and held at this temperature for 20–30 min.

Compound specific stable carbon isotope ratios were determined by Finnigan Mat Delta Plus mass spectrometer interfaced to a HP 5890II gas chromatograph. Gas components were separated on the GC using helium as the carrier gas, converted into $CO_2$ in a combustion interface, and then introduced into the mass spectrometer. Individual hydrocarbon gas components ($C_1$–$C_5$) and $CO_2$ were initially separated using a fused silica capillary column (PLOT Q 30 m × 0.32 mm). The GC oven temperature was increased from

**Table 2**
Gas geochemical characteristics of shale gases liberated in the desorption experiments.

| Sample and desorption step | | Temp. | Yield (mL/g) | Gas composition (%) | | | | | | | $C_1/C_{1-5}$ | $\delta^{13}C$ (‰) | | | | | $\delta^2H$ (‰) | |
|---|---|---|---|---|---|---|---|---|---|---|---|---|---|---|---|---|---|---|
| | | | | $CH_4$ | $C_2H_6$ | $C_3H_8$ | $iC_4H_{10}$ | $nC_4H_{10}$ | $iC_5H_{12}$ | $nC_5H_{12}$ | | $CH_4$ | $C_2H_6$ | $C_3H_8$ | $nC_4H_{10}$ | $CO_2$ | $CH_4$ | $C_2H_6$ |
| YY5–1 | 1 | 20 °C | 0.377 | 65.71 | 10.57 | 5.01 | 0.48 | 0.94 | 0.13 | 0.14 | 0.792 | −51.6 | −37.8 | −32.1 | −30.0 | −16.1 | −264.3 | −229.8 |
| | 2 | 20 °C | 0.177 | 51.79 | 8.52 | 4.48 | 0.50 | 0.87 | 0.14 | 0.12 | 0.780 | −49.3 | −37.3 | −32.4 | −30.3 | −17.9 | −255.1 | −222.9 |
| | 3 | 20 °C | 0.099 | 60.52 | 10.10 | 5.33 | 0.62 | 1.00 | 0.16 | 0.15 | 0.777 | −50.1 | −37.4 | −32.0 | −29.8 | −18.9 | −264.4 | −227.9 |
| | 4 | 40 °C | 0.255 | 61.53 | 12.63 | 7.24 | 0.80 | 1.73 | 0.29 | 0.35 | 0.727 | −50.2 | −37.7 | −32.4 | −30.2 | −15.3 | −263.8 | −230.2 |
| | 5 | 60 °C | 0.221 | 52.46 | 13.79 | 8.89 | 1.07 | 2.40 | 0.45 | 0.57 | 0.659 | −48.1 | −37.0 | −32.3 | −31.1 | −14.6 | −264.3 | −232.3 |
| | 6 | 70 °C | 0.158 | 33.11 | 10.61 | 7.17 | 0.91 | 1.73 | 0.33 | 0.40 | 0.610 | −42.4 | −34.8 | −31.1 | −30.1 | −20.7 | −258.5 | −229.6 |
| | 7 | 80 °C | 0.077 | 27.35 | 11.03 | 8.35 | 1.17 | 2.17 | 0.45 | 0.54 | 0.536 | −40.9 | −35.2 | −31.7 | −30.7 | −17.1 | −257.8 | −229.6 |
| | 8 | 90 °C | 0.050 | 19.29 | 10.48 | 8.49 | 1.27 | 2.09 | 0.45 | 0.59 | 0.452 | −33.9 | −33.5 | −31.1 | −30.3 | −18.4 | −251.9 | −227.4 |
| YY5–2 | 1 | 20 °C | 0.264 | 69.80 | 10.65 | 4.90 | 0.46 | 0.85 | 0.12 | 0.12 | 0.803 | −51.6 | −37.7 | −32.1 | −36.7 | −14.5 | −265.2 | −225.3 |
| | 2 | 20 °C | 0.136 | 61.82 | 9.97 | 4.88 | 0.50 | 0.87 | 0.12 | 0.13 | 0.790 | −51.3 | −37.8 | −32.4 | −28.9 | −19.0 | −263.4 | −221.7 |
| | 3 | 20 °C | 0.081 | 65.63 | 10.12 | 5.12 | 0.56 | 0.91 | 0.14 | 0.13 | 0.794 | −51.0 | −37.5 | −32.3 | −30.4 | −16.9 | −263.9 | −227.0 |
| | 4 | 40 °C | 0.215 | 64.68 | 12.20 | 6.74 | 0.71 | 1.57 | 0.25 | 0.30 | 0.748 | −51.3 | −37.9 | −32.7 | −31.5 | −15.7 | −263.8 | −230.2 |
| | 5 | 60 °C | 0.358 | 61.29 | 14.15 | 8.29 | 0.87 | 2.12 | 0.35 | 0.50 | 0.700 | −49.7 | −37.8 | −32.8 | −31.5 | −16.2 | −264.3 | −232.9 |
| | 6 | 70 °C | 0.189 | 37.00 | 10.29 | 6.86 | 0.84 | 1.70 | 0.31 | 0.35 | 0.645 | −45.2 | −36.4 | −31.8 | −30.1 | −17.2 | −256.5 | −226.7 |
| | 7 | 80 °C | 0.125 | 31.04 | 10.53 | 7.34 | 0.93 | 1.85 | 0.34 | 0.42 | 0.592 | −41.9 | −35.6 | −31.8 | −30.1 | −23.3 | −256.4 | −224.3 |
| | 8 | 90 °C | 0.066 | 26.97 | 12.48 | 9.79 | 1.37 | 2.53 | 0.51 | 0.68 | 0.496 | −36.0 | −34.0 | −31.2 | −30.4 | −19.1 | −249.8 | −226.4 |

**Table 3**
Chemical and stable carbon and hydrogen isotopic compositions of the shale gases and conventional gas in the Yanchang formation, Ordos Basin.

| Field | Well | Reservoir types | Deep (m) | $\delta^{13}C$ (‰) | | | $\delta^{2}H$ (‰) | | Gas composition (%) | | | | | $C_1/C_{1-5}$ |
|---|---|---|---|---|---|---|---|---|---|---|---|---|---|---|
| | | | | $CH_4$ | $C_2H_6$ | $C_3H_8$ | $CH_4$ | $C_2H_6$ | $CH_4$ | $C_2H_6$ | $C_3H_8$ | $iC_4H_{10}$ | $nC_4H_{10}$ | |
| Xiasiwan | X57 | Shale gas | 1240–1252 | −48.1 | −36.7 | −32.4 | n.d. | n.d. | 68.25 | 11.52 | 7.18 | 0.98 | 2.10 | 0.76 |
| | X59 | reservoir | 1076–1084 | −46.6 | −36.1 | −31.4 | n.d. | n.d. | 74.16 | 8.47 | 5.90 | 1.01 | 2.17 | 0.81 |
| | LP177 | | 1470–1505 | −48.2 | −34.4 | −30.7 | −242.8 | −221.2 | 88.07 | 5.27 | 1.92 | 0.32 | 0.39 | 0.92 |
| | LP179 | | 1453–1470 | −47.5 | −35.9 | −30.8 | −247.2 | −208.4 | 83.42 | 6.80 | 3.08 | 0.44 | 0.76 | 0.88 |
| | LU63 | Conventional | 1366–1384 | −47.8 | −36.3 | −31.7 | −257.1 | −220.8 | 74.35 | 10.64 | 6.47 | 0.89 | 1.90 | 0.79 |
| | LU65 | reservoir | 669–671 | −50.9 | −36.1 | −31.7 | −255.3 | −216.5 | 68.41 | 8.50 | 5.79 | 0.88 | 1.50 | 0.80 |
| | Z28 | | 1356–1364 | −47.1 | −31.1 | −30.1 | n.d. | n.d. | 94.56 | 1.50 | 0.56 | 0.24 | 0.21 | 0.97 |
| Yongning | S23 | Conventional | 1213–1233 | −49.9 | −38.8 | −34.4 | −280.0 | −244.5 | 71.22 | 11.06 | 7.71 | 0.77 | 1.85 | 0.77 |
| | S109 | reservoir | 1409–1424 | −49.7 | −38.4 | −34.1 | −280.2 | −244.1 | 75.67 | 10.20 | 6.07 | 0.53 | 1.26 | 0.81 |
| | SE4 | | 1523–1546 | −49.9 | −38.9 | −34.3 | −281.1 | −254.4 | 78.84 | 9.00 | 4.88 | 0.40 | 0.89 | 0.84 |
| Dingbian | D3171 | | 1778–1782 | −43.4 | −36.1 | −33.9 | n.d. | n.d. | 30.11 | 7.43 | 12.05 | 1.80 | 3.56 | 0.55 |
| | D3166 | | 1796–1798 | −42.9 | −35.8 | −33.2 | n.d. | n.d. | 49.53 | 11.06 | 13.55 | 1.74 | 3.14 | 0.63 |
| | D3172 | | 1776–1779 | −43.2 | −35.9 | −33.6 | n.d. | n.d. | 39.71 | 10.91 | 19.53 | 2.76 | 5.01 | 0.51 |
| Yingwang | L95 | | 678–680 | −44.6 | −34.7 | −31.8 | −256.7 | −225.3 | 62.41 | 9.76 | 5.89 | 0.99 | 1.36 | 0.78 |
| | L87-2 | | 688–689.5 | −44.8 | −35.0 | −32.0 | −256.6 | −228.0 | 61.90 | 10.44 | 6.86 | 1.16 | 1.87 | 0.75 |
| | N14 | | 727.2–729.2 | −44.8 | −34.4 | −31.8 | −248.8 | −227.7 | 53.83 | 12.54 | 10.45 | 2.11 | 3.55 | 0.65 |
| | N9 | | 665.5–666.5 | −44.4 | −34.4 | −31.7 | −249.2 | −226.7 | 60.51 | 12.16 | 8.13 | 1.37 | 2.13 | 0.72 |

35 °C to 80 °C at 8 °C/min, then to 260 °C at 5 °C/min, and held there for 10 min. Stable isotope ratios for carbon are reported in $\delta$ notation in per mil (‰) relative to VPDB. The measurement precision was estimated to be ±0.5‰ for $\delta^{13}C$.

Compound-specific hydrogen stable isotope ratios were measured by Finnigan Mat Delta Plus mass spectrometer interfaced with a HP 5890II gas chromatograph. Gas components were separated on a HP-PLOT Q column (30 m × 0.32 mm × 20 μm) with helium as the carrier gas (1.5 mL/min). A split injection was used for methane with a split ratio of 1:7 at 40 °C. For the analysis of ethane and propane, the gas was introduced via splitless injection. The GC oven temperature was initially set to 40 °C for 4 min, then increased to 80 °C at 10 °C/min, then to 140 °C at 5 °C/min, and finally to 260 °C°C at 30 °C/min. The precision was ±3‰ with respect to VSMOW.

## 3. Results

### 3.1. Geochemical characteristics of the natural gas

The chemical compositions and stable carbon/hydrogen isotope composition of natural gases from the Triassic Yanchang Formation are given in Table 3. Within the study area, the shales with high total organic carbon content (TOC) are mainly distributed in the Xiasiwan and Yongning Fields in which the TOC is 2–5% and the Ro is 1.0–1.2% (Fig. 1). At present, most of the identified shale gas reservoirs are found within the Xiasiwan Field. The geochemical characteristics of the shale gas show unconspicuous differences compared to those of the conventional natural gas in the Xiasiwan Field, and the methane is depleted in $^{13}C$ in both ($\delta^{13}C_1$ = −50.9‰ to −46.6‰). The geochemical characteristics of conventional gas reservoirs in Yongning Field are basically identical to those of Xiasiwan, and there is currently no shale gas exploration or development in Yongning Field. The properties of the shales in Dingbian and Yingwang Fields are not as attractive. In these areas, the TOC ranges of 1–2% and the Ro ranges of 0.5–1.0% (Fig. 1). Although the maturity of shale is low in Dingbian and Yingwang Fields, their $\delta^{13}C_1$ (−44.8‰ to −42.9‰) is relatively enriched in $^{13}C$ compared to those found in the Xiasiwan and Yongning areas (Fig. 3, Table 3).

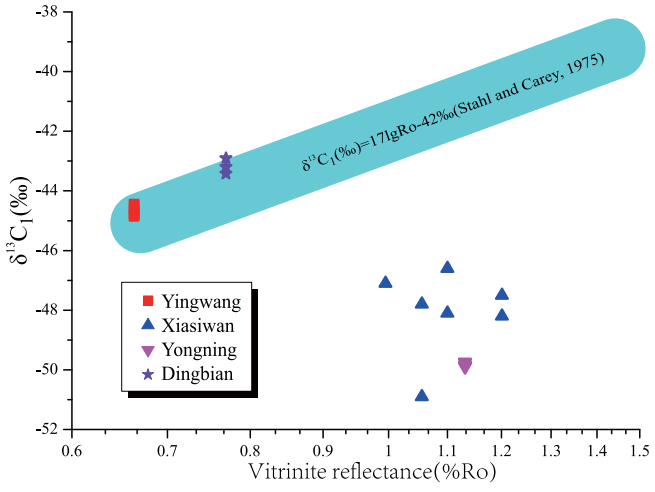


**Figure 3.** The methane in the natural gas samples of the Xiasiwan and Yongning areas is isotopically depleted in $^{13}C$ than predicted by the relationship between $\delta^{13}C_1$ and Ro of Stahl and Carey (1975). The shales with good properties are mainly distributed in those areas.

### 3.2. Geochemical characteristics of the desorbed gas

The liberation rate of the shale gas decreased gradually during desorption at room temperature (20 °C); it increased rapidly as the

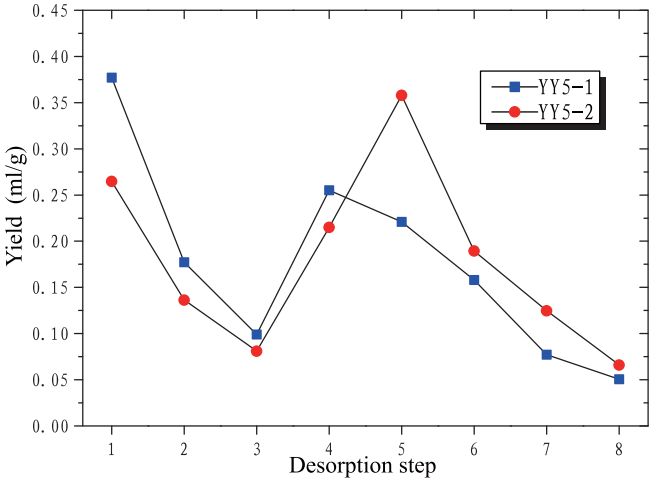


**Figure 4.** The liberation rate of the shale gas decreased gradually during desorption at room temperature (20 °C); it increased rapidly as the temperature rose to 40 °C, then decreased gradually as the temperature was raised to 90 °C. The desorption yield of the two shale samples in the experiments were measured to be 1.415 mL/g and 1.435 mL/g respectively.

temperature rose to 40 °C, then decreased gradually as the temperature was raised to 90 °C (Fig. 4). The dryness coefficient ($C_1/C_{1-5}$) of gases desorbed from the shale gradually dropped from 0.8 in the first desorption step to 0.5 in the last step (Fig. 5a). This is due to the fact that smaller molecules, like methane, desorb more rapidly than longer chain hydrocarbons. A relatively large change in the $\delta^{13}C_1$ values, from −51.6‰ to −33.9‰, is observed with increasing degree of desorption (Fig. 5b). In contrast, the $\delta^{13}C$ values of ethane and propane changed less (4‰ and 1‰, respectively), and the $\delta^{13}C$ values of butane and $CO_2$ showed unidentifiable change throughout the desorption sequence (Fig. 5c–f). The hydrogen isotopic ratio of methane ($\delta^2H_{C1}$) also changed with increasing degree of desorption, becoming more enriched in D (from −265.2‰ to −249.8‰; Fig. 5g). For the hydrogen isotopic ratio of ethane ($\delta^2H_{C2}$) no regular change is observed in any of the desorption experiments (Fig. 5h).

## 4. Discussion

### 4.1. Carbon isotopic composition of shale gases

The relationship between $\delta^{13}C_1$ and Ro in conventional natural gases is well established and widely accepted and it plays an essential part in the research on gas geochemistry. However, such relationship models are inapplicable for shale gas, or even for conventional gas in shale gas regions.

Development of shale gas began in the United States, with the Barnett Shale in the Fort Worth Basin being one of the most successful exploration targets. Barnett Shale gas maturities determined from isotope analysis support thermal generation of oil and gas, with some gas possibly generated by the cracking of oil (Montgomery et al., 2005). Preliminary screening of the molecular composition and $\delta^{13}C_1$ of the Barnett Shale gases (Rodriguez and Philp, 2010; Zumberge et al., 2012) allows the identification of two main groups. Group 1 is composed mainly of gas samples with a $\delta^{13}C_1$ more positive than −42‰ (from −42‰ to −37‰) and a wetness < 5% (average $C_1/C_{1-5}$ of 0.974). Those samples are mainly distributed in regions with relatively high levels of shale maturity (Ro = 1.3–1.7%), with some samples showing isotope reversals ($\delta^{13}C_1 > \delta^{13}C_2$) (Rodriguez and Philp, 2010; Zumberge et al., 2012). The $\delta^{13}C_1$ of group 1 was isotopically depleted in $^{13}C$ than that calculated by Ro according to Stahl and Carey's $\delta^{13}C_1$–Ro equation (Fig. 6). Group 2 is composed mainly of gas samples with a wetness >7% (average $C_1/C_{1-5}$ of 0.832) and a $\delta^{13}C_1$ more negative than −42‰ (from −48‰ to −42‰). Samples from group 2 mainly are found in regions with relatively low shale maturity (Ro = 1.1–1.3%). The $\delta^{13}C_1$ of group 2 was also obviously depleted in

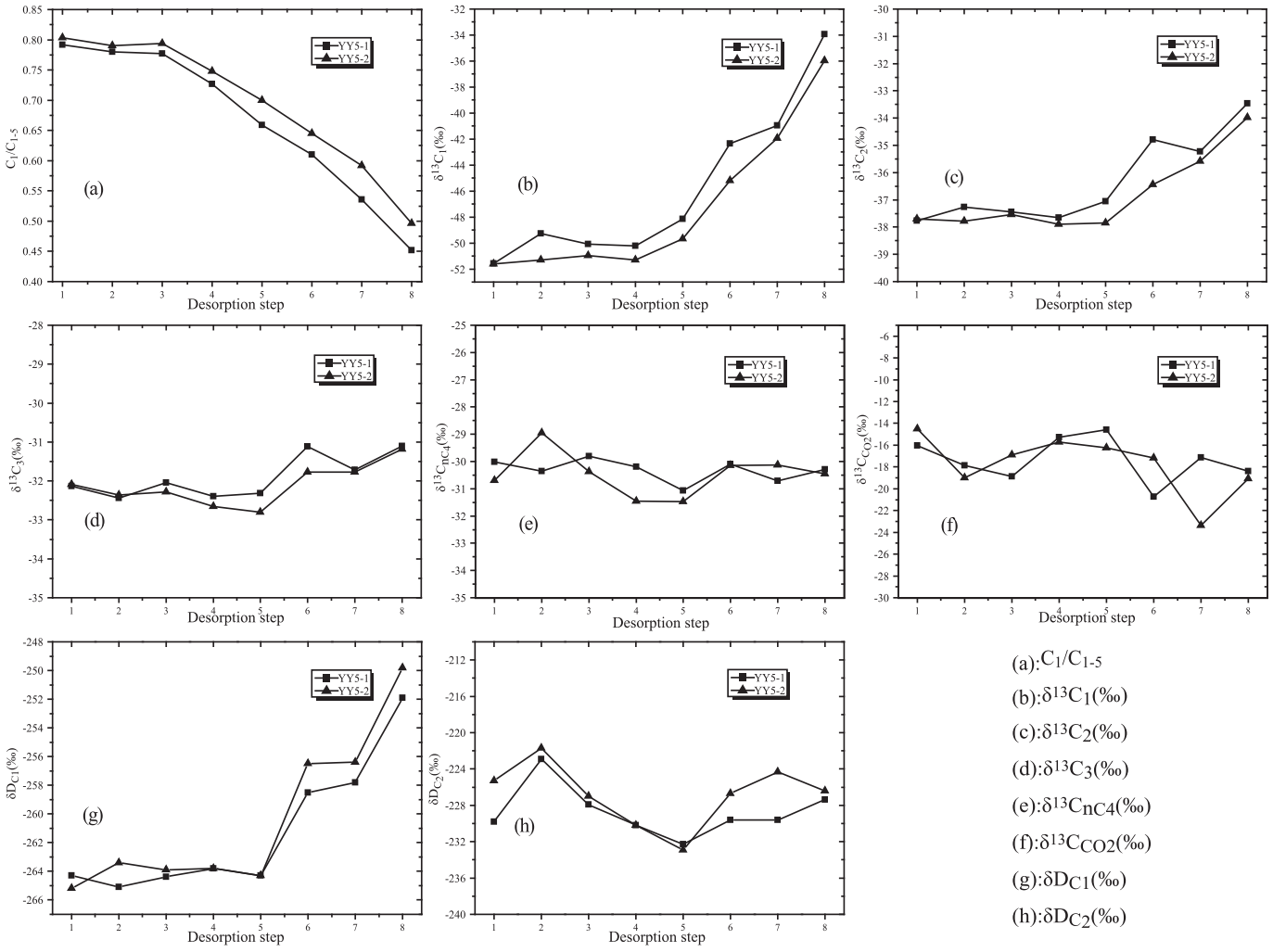


**Figure 5.** Plots of various gas geochemical parameter changes in the desorption experiments. The carbon and hydrogen isotopic composition of methane become more negative as the desorption time increased. In contrast, the carbon isotopic composition of ethane and propane changed less, and the $\delta^{13}C$ of butane and $CO_2$ had no identifiable change in any of the desorption experiments. The hydrogen isotopic composition of ethane ($\delta^2H_{C2}$) has no observable change in any of the desorption experiments.

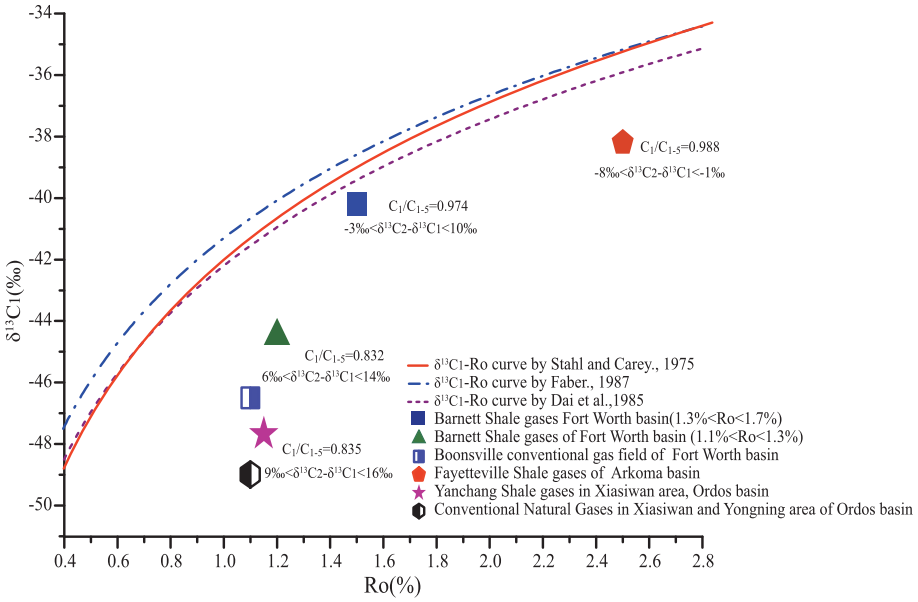


**Figure 6.** The lines show the relationship between $\delta^{13}C_1$ and Ro in conventional natural gas. Many researchers proposed the regression equation, but the differences between them are very small. But such relationship models are not applicable for shale gas, or even for conventional gas in shale gas regions. The dynamic changes of geochemical characteristics in shale gas systems maybe a main reason. The Yanchang and Barnett shale gases show the largest isotopic fractionation.

$^{13}C$ compared with the maturity of shale (Fig. 6). Gas is generally dryer with higher maturity and that real gas generation starts after 0.9%Ro for sapropelic organic matter. The Boonsville gas field is a conventional reservoir which lies within a shale gas region. Analysis of gas samples from the Pennsylvanian Boonsville conglomerate reservoir unit suggests that it is sourced by the Barnett Shale (Pollastro et al., 2007). Reservoirs of the Boonsville conglomerate were probably the first to receive gas generated by the Barnett source rocks (Hill et al., 2007). Gas in the Boonsville conglomerate is wetter and has a lower thermal maturity than gas produced from the Barnett Shale (Pollastro et al., 2007). The $\delta^{13}C_1$ of the Boonsville gas field was also obviously depleted in $^{13}C$ compared with the maturity of shale (Fig. 6).

The Triassic Yanchang Formation in the Ordos Basin became known as China's first terrestrial shale gas well. Gas in the Yanchang Shale is wet and the $\delta^{13}C_1$ value is generally higher than −50‰, which means that there is almost no contribution from biogenic gas. The Yanchang Formation has been buried (>2500 m) and uplifted later. Transient exposure to higher temperatures may "sterilize" strata. Furthermore, once sterilized, strata are not recolonized by microbes (Peters et al., 2005). Whether or not microbes can be introduced into reservoirs by subsurface aqueous flow has yet to be resolved; for example, microbes may be too large to move through many fine-grained rocks, such as shale (Peters et al., 2005). Therefore, there is no doubt that the shale gas of Yanchang Formation is thermogenic. However, the similar problems need to be faced concerning the obvious discrepancy between (a) shale gas and conventional gas in Xiasiwan and Yongning area with a $\delta^{13}C_1$ depleted in $^{13}C$ (−48.0‰ average) and (b) the thermal maturity of the shale (Ro ≈ 1.1%).

### 4.2. The reasons for more negative $\delta^{13}C_1$ of shale gas

It is widely acknowledged that coal bed methane (CBM) mainly exists in a state of adsorption, with the adsorbed gas generally between 80% and 90% of the total gas content, and the $\delta^{13}C_1$ of CBM generally is depleted in $^{13}C$ than that of gases in terrestrial organic matter sourced gas fields with a similar coal rank (Qin et al., 2006). The proportion of adsorbed gas (the important form of shale gas) is generally between 20% and 85% in shale gas. Shale gases and CBM are different from conventional gas because of the proportion of the gas that exists in an adsorbed state, which leads to a great difference in development theory. Besides, the geochemical fractionation during an adsorption/desorption process may play a more important role for the more negative $\delta^{13}C_1$ of shale gas and CBM. Su et al. (2007) indicated that the adsorption potential of $^{13}CH_4$ in coal is greater than that of $^{12}CH_4$, and its effect is more obvious in higher pressure.

Desorption experiments show that $\delta^{13}C_1$ of desorbed gas changes little in the first few phases but increases rapidly when the fraction of desorbed methane exceeds 85% (Fig. 7). The desorption process for the last 15% of the methane from the shale samples shows a wide variation in $\delta^{13}C_1$ from −49‰ to −33.9‰. This is very different to the $\delta^{13}C_1$ fractionation model caused by diffusion (Zhang and Krooss, 2001). The cumulative $\delta^{13}C_1$ values of the total methane desorbed from the two shale samples are −49.2‰ and −49.6‰ respectively, which is much depleted in $^{13}C$ than that calculated from Ro according to Stahl and Carey's $\delta^{13}C_1$–Ro equation.

The $\delta^{13}C_1$–Ro equations are derived from large amounts of data statistics, and they play an important part in conventional gas geochemistry research. We have reason to believe that those equations should also apply to shale gas, because the hydrocarbon generation mechanism for shale gas is similar to that of conventional gas. Some gas may have migrated out of the shale before shale gas development, but there is no evidence for that the $\delta^{13}C_1$ of these gases was more enriched in $^{13}C$. Additionally, we also found that $\delta^{13}C_1$ of conventional gases is depleted in $^{13}C$ in shale gas region, such as Boonsville conglomerate reservoir in Barnett shale gas region. On the other hand, some gases dissipate in the course of drilling. Nevertheless, the $\delta^{13}C_1$ of the lost gases should be depleted in $^{13}C$ too.

The desorption yields of the two shale samples in the experiments were measured to be 1.415 mL/g and 1.435 mL/g respectively. Some gas still remains in the shale and it cannot be desorbed under the temperature and pressure conditions of the experiments. According to the $\delta^{13}C_1$ trends for the desorption process, the $\delta^{13}C_1$ of this part of the gas should be more positive, although the amount of

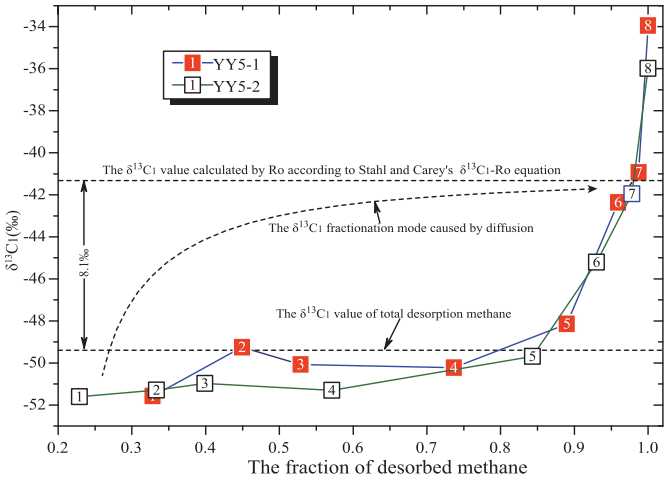


**Figure 7.** The $\delta^{13}C_1$ changes little in the first few phases of the experiments then increases rapidly as the fraction of desorbed methane exceeds 85%. There is a 8.1‰ deviation between the $\delta^{13}C_1$ value of totally desorbed methane and that calculated by Ro according to $\delta^{13}C_1$–Ro equation. Carbon isotopic fractionation by diffusion mainly reflected in the early stages of the experiment. This model is very different to the $\delta^{13}C_1$ fractionation caused by diffusion.

this part is not great. We believe that this proportion of the gas cannot be desorbed during shale gas development either.

Many previous investigations have indicated that the adsorption/desorption effects make the $\delta^{13}C_1$ of CBM more negative. However, this explanation raises many questions. Qin et al. (2006) point out that if the more negative $\delta^{13}C_1$ in the desorbed belt were caused by CBM desorption from original belt, then the remaining CBM in original belt would be enrich in $^{13}C$ because the $^{12}CH_4$ would be desorbed first, prior to the $^{13}CH_4$. In fact, it is unquestionable that CBM are generally depleted in $^{13}C$ than that of gas in normal coal-formed gas fields of similar source maturity whether desorbed belt or original belt. So he thought more negative $\delta^{13}C_1$ of CMB is caused by other factors (Qin et al., 2006). But this point could be problematic judged from the evidence provided by the desorption experiments in this paper. The reason to suspect this is that there is some CBM with greater $\delta^{13}C$ value in coal which cannot be permanently desorbed during the development of CBM. So the $\delta^{13}C_1$ of CBM which we can analyze by conventional means is always more negative compared to conventional gas of similar source maturity whether in the desorbed belt or original belt.

### 4.3. A geological explanation for the shale gas geochemistry

For the adsorption/desorption process, recent research indicates that gas is distributed dominantly as free gas and adsorbed gas in the nanopores of an organic matrix (Ross and Bustin, 2009). The polar surfaces of clay minerals are generally wetted with water, so adsorption of methane on clays can be neglected (Xia and Tang, 2012). The adsorption capacity of coal is far stronger than shale because coal has a greater abundance of organic matter than shale. Moreover, the fractionation of $\delta^{13}C$ in shale gas systems is far less than in CBM, according to the presented information. Therefore, the magnitude of the deviation between the $\delta^{13}C_1$ of shale gas and that calculated by Ro may be related to the adsorption capacity of shale or the proportion of absorbed gases. In this way, we may be able to evaluate the relative adsorption capacity of shale in geological conditions by $\delta^{13}C_1$ of the shale gas, or by $\delta^{13}C_1$ of conventional gas which generated by the shale with certainty.

The gas geochemistry of the Yanchang Formation is well understood, as shown in the above discussion. The reason that gases, including shale gases and conventional gases, have a more negative $\delta^{13}C_1$, is that the shale has a higher organic matter abundance (TOC of 2–5%) and thickness in Xiasiwan and Yongning Fields. These conditions enable the shale to have a higher adsorption capacity for methane, which leads to the more negative $\delta^{13}C_1$ of desorbed gas. Accordingly, because the carbon and hydrogen isotopic composition in the Yongning area more negative, there is good potential for shale gas development, even though there has been no shale gas development implemented in that region yet.

## 5. Conclusion

The geochemical characteristics of the shale gas show unconspicuous differences compared to those of the conventional natural gas in the Xiasiwan and Yongning Fields, and the methane is depleted in $^{13}C$ in both ($\delta^{13}C_1 = -50.9‰$ to $-46.6‰$). Although the maturity is low in Dingbian and Yingwang Fields, their $\delta^{13}C_1$ ($-44.8‰$ to $-42.9‰$) of gases generated from the shale is relatively enriched in $^{13}C$ compared to those found in the Xiasiwan and Yongning Fields.

There is a well-constrained relationship between $\delta^{13}C_1$ and Ro in conventional natural gases. However, this relationship is not applicable for shale gas, or even for conventional gas in Xiasiwan and Yongning Fields. The geochemical characteristics of shale gases show that the $\delta^{13}C_1$ is generally depleted in $^{13}C$ than that calculated by Ro according to the $\delta^{13}C_1$–Ro equation. The fractionation of geochemical parameters during the adsorption/desorption process play an essential role in the more negative $\delta^{13}C_1$ of shale gas.

Desorption experiments show that $\delta^{13}C_1$ changes little in the first few phases of the experiments at low desorption levels, but increases rapidly when the fraction of desorbed methane exceeds 85%. The $\delta^{13}C_1$ value for all desorbed methane from two shale samples is also depleted in $^{13}C$ than that calculated by Ro according to $\delta^{13}C_1$–Ro equation. This difference shows that there are some gases with a less negative $\delta^{13}C$ in the shale that cannot be desorbed. The magnitude of the deviation between the $\delta^{13}C_1$ of shale gas and that calculated by Ro may be related to the adsorption capacity of shale or the proportion of absorbed gases. We may be able to assess the relative adsorption capacity of shale in geological conditions by $\delta^{13}C_1$ of the shale gas, or by $\delta^{13}C_1$ of conventional gas which generated by the shale with certainty.

## Acknowledgments

This study was supported by National Nature Science Foundation of China (Grant No. 41372156), the Major National R&D Projects (Grant No. 2011ZX05008–004) and the Key Laboratory Project of Gansu Province (Grant No.1309RTSA041). We are grateful to Thomas Hantschel, William Meredith and an anonymous reviewer for their helpful comments and contributions that allowed us to improve the manuscript.

## References

Berner, U., Faber, E., 1996. Empirical carbon isotope/maturity relationships for gases from algal kerogen and terrigenous organic matter, based on dry, open-system pyrolysis. Org. Geochem. 24, 947–955.

Burruss, R.C., Laughrey, C.D., 2010. Carbon and hydrogen isotopic reversals in deep basin gas: evidence for limits to the stability of hydrocarbons. Org. Geochem. 41, 1285–1296.

Chung, H.M., Gormly, J.R., Squires, R.M., 1988. Origin of gaseous hydrocarbons in subsurface environments: theoretical considerations of carbon isotope distribution. Chem. Geol. 71, 97–103.

Claypool, G.E., 1998. Kerogen conversion in fractured shale petroleum systems. Am. Assoc. Pet. Geol. Bull. 82. Supplment 5.

Cramer, B., Krooss, B.M., Littke, R., 1998. Modeling isotope fractionation during primary cracking of natural gas: a reaction kinetic approach. Chem. Geol. 149, 235–250.

Dai, J.X., Qi, H.F., 1989. The $\delta^{13}C$–Ro relation of coal-formed hydrocarbon in China. Chin. Sci. Bull. 34, 110–113 (in Chinese).
Faber, E., 1987. Zur Isotopengeochemie gasförmiger Kohlen-wasserstoffe. Erdöl Erdgas Kohle Z 1035, 210–218.
Hill, R.J., Jarvie, D.M., Zumberge, J., Henry, M., Pollastro, R.M., 2007. Oil and gas geochemistry and petroleum systems of the Fort Worth Basin. Am. Assoc. Pet. Geol. Bull. 91, 445–473.
Jarvie, D.M., 2007. Unconventional shale-gas systems; the Mississippian Barnett Shale of north-central Texas as one model for thermogenic shale-gas assessment. Am. Assoc. Pet. Geol. Bull. 91, 475–499.
Liu, W.H., Chen, M.J., Guan, P., Zheng, J.J., Jin, Q., Li, J., Wang, W.C., Hu, G.Y., Xia, Y.Q., Zhang, D.W., 2007. Ternary geochemical-tracing system in natural gases accumulation. Sci. China Ser. D 50, 1494–1503.
Martini, A.M., Walter, L.M., Budai, J.M., Ku, T.C.W., Kaiser, C.J., Schoell, M., 1998. Genetic and temporal relations between formation waters and biogenic methane—Upper Devonian Antrim Shale, Michigan basin, USA. Geochim. Cosmochim. Acta 62, 1699–1720.
Montgomery, S.L., Jarvie, D.M., Bowker, K.A., Pollastro, R.M., 2005. Mississippian Barnett Shale, Fort Worth basin, north-central Texas: gas-shale play with multi-trillion cubic foot potential. Am. Assoc. Pet. Geol. Bull. 89, 155–175.
Osborn, S.G., McIntosh, J.C., 2010. Chemical and isotopic tracers of the contribution of microbial gas in Devonian organic-rich shales and reservoir sandstones, northern Appalachian Basin. Appl. Geochem. 25, 456–471.
Peters, K.E., Walters, C.C., Moldowan, J.M., 2005. The Biomarker Guide, second ed. Cambridge University Press, New York, pp. 645–708.
Pollastro, R.M., Jarvie, D.M., Hill, R.J., Adams, C.W., 2007. Geologic framework of the Mississippian barnett shale, Barnett-Paleozoic total petroleum system, Bend arch–Fort Worth Basin, Texas. Am. Assoc. Pet. Geol. Bull. 91, 405–436.
Qin, S., Tang, X., Song, Y., Wang, H., 2006. Distribution and fractionation mechanism of stable carbon isotope of coalbed methane. Sci. China Ser. D Earth Sci. 49, 1252–1258.
Rodriguez, N.D., Philp, R.P., 2010. Geochemical characterization of gases from the Mississippian barnett shale, fort Worth Basin, Texas. Am. Assoc. Pet. Geol. Bull. 94, 1641–1656.
Ross, D.J.K., Bustin, R.M., 2009. The importance of shale composition and pore structure upon gas storage potential of shale gas reservoirs. Mar. Pet. Geol. 26, 916–927.
Schettler, P.D., Parmely, C.R., 1990. The measurement of gas desorption isotherms for Devonian shale. Gas. Shales Technol. Rev. 7, 4–9.
Schoell, M., 1980. The hydrogen and carbon isotopic composition of methane from natural gases of various origins. Geochim. Cosmochim. Acta 44, 649–661.
Schoell, M., 1983. Genetic characterization of natural gasses. Am. Assoc. Pet. Geol. Bull. 67, 2225–2238.
Schoell, M., 1988. Multiple origins of methane in the earth. Chem. Geol. 71, 1–10.
Shen, P., Shen, Q., Wang, X., Xu, Y., 1988. Characteristics of the isotope composition of gas-form hydrocarbons and the identification of coal-type gas. Sci. China, Ser. B 31, 242–249.
Stahl, W.J., Carey, J.B.D., 1975. Source-rock identification by isotope analyses of natural gases from fields in the Val Verde and the Delaware Basin, West Texas. Chem. Geol. 16, 257–267.
Stahl, W.J., 1977. Carbon and nitrogen isotopes in hydrocarbon research and exploration. Chem. Geol. 20, 121–149.
Su, X., Chen, R., Lin, X., Guo, S., 2007. The adsorption characteristic curves of $^{13}CH_4$ and $^{12}CH_4$ on coal and its application. J. China Coal Soc. 32, 539–543 (in Chinese with English abstract).
Tang, Y., Perry, J.K., Jenden, P.D., Schoell, M., 2000. Mathematical modeling of stable carbon isotope ratios in natural gases. Geochim. Cosmochim. Acta 64, 2673–2687.
Tilly, B., McLellan, S., Hiebert, S., 2011. Gas isotope reversals in fractured gas reservoirs of the western Canadian Foothills: mature shale gases in disguise. Am. Assoc. Pet. Geol. Bull. 95, 1399–1422.
Tilly, B., Muehlenbachs, K., 2013. Isotope reversals and universal stages and trends of gas maturation in sealed, self-contained petroleum systems. Chem. Geol. 339, 194–204.
Xia, X., Chen, J., Braun, R., Tang, Y., 2013. Isotopic reversals with respect to maturity trends due to mixing of primary and secondary products in source rocks. Chem. Geol. 339, 205–212.
Xia, X., Tang, Y., 2012. Isotope fractionation of methane during natural gas flow with coupled diffusion and adsorption/desorption. Geochim. Cosmochim. Acta 77, 489–503.
Xu, Y., 1994. Genetic Theory of Natural Gases and its Application. Science Press, Beijing, pp. 122–146 (in Chinese).
Zhang, T., Krooss, B.M., 2001. Experimental investigation on the carbon isotope fractionation of methane during gas migration by diffusion through sedimentary rocks at elevated temperature and pressure. Geochim. Cosmochim. Acta 65, 2723–2742.
Zumberge, J., Ferworn, K., Brown, S., 2012. Isotopic reversal ('rollover') in shale gases produced from the Mississippian Barnett and Fayetteville formations. Mar. Pet. Geol. 31, 43–52.